1 **Abnormal mitochondrial functional markers in a rat model of "kidney yang deficiency" and**

2 **related metabolic disorders**

3

4 Haiyang Cai[1]*, Xiaomin Huang[2]*, Han Li[1]*, George Herok[3], Jing He[1], Yixun Su[2], Weihong Li[1],

5 Chenju Yi[2†], Brian G Oliver[3], Hui Chen[3†]

6 * Equal contributions

7

8 1. Faculty of Basic Medical Sciences, Chengdu University of Traditional Chinese Medicine, Chengdu,

9 Sichuan, China

10 2. The Seventh Affiliated Hospital of Sun Yat-Sen University, Shenzhen, China

11 3. School of Life Sciences, University of Technology Sydney, Sydney, NSW, Australia

12

13 † Corresponding authors:

14 Associate Professor Chenju Yi, yichj@mail.sysu.edu.cn

15 Associate Professor Hui Chen, hui.chen-1@uts.edu.au

16

18

Abstract

The mitochondrion is the cellular 'powerhouse', generating ATP to support all physiological functions and maintain core body temperature. In Chinese Medicine, the kidney is also considered as the body's 'powerhouse', in which a common pattern called Kidney Yang Deficiency (KYD) describes a series of conditions suggesting energy shortage, eg. cold intolerance, fatigue, and labor intolerance, with reduced blood corticosterone levels. We hypothesized that KYD may be linked to impaired mitochondrial function in thermogenesis and metabolic tissues, therefore making them also prone to metabolic disorders. A rat model of KYD was used, which was established using Sprague Dawley rat dams with warm preference subjected to herbal treatment that can suppress Kidney Yang. The human relevance was confirmed by reduced serum corticosterone levels, and increased preference for warm location. KYD Rats were underdeveloped. ATP production was reduced in the brown fat, but increased in the muscle. However, oxidative phosphorylated complexes to generate ATP and mitochondrial biogenesis marker were reduced in both tissues. When the second insult of high-fat diet (HFD) was introduced, KYD rats gained less weight yet developed more severe lipid and glucose metabolic disorders. This may be driven by dysregulated liver gluconeogenesis marker FOXO1 and lipid metabolic regulator CYP7A1. In conclusion, KYD rats exhibited reduced mitochondrial function in the brown fat, but were partially compensated by skeletal muscle, associated with the phenotype of warm preference and metabolic disorder, which was further exacerbated by additional HFD consumption. Future studies can focus on treatment targeting mitochondria function to reverse this phenotype.

1. Introduction

The mitochondrion is the cellular 'powerhouse', which is essential to generate the energy substance ATP to support all physiological functions. The heat generated during this process also contributes to the maintenance of core body temperature. As such, mitochondrial density is higher in energy-demanding and heat-generating organs, such as the skeletal muscle and brown adipose tissue (BAT) (Chan et al., 2020). The production of ATP through oxidative phosphorylation (OXPHOS) takes place at the cristae of the mitochondrion and is facilitated by OXPHOS complexes I-V. OXPHOS Complex(C) I is an L shaped protein that acts as the first entry point of electrons in the respiratory chain. OXPHOS CII is the second entry for electrons to the respiratory chain. OXPHOS CIII facilitates electron transfer to OXPHOS CIV. The generated protons from OXPHOS CI to CIV drive ATP synthase in OXPHOS CV (Dudkina et al., 2010). Mitochondrial dysfunction has been found to contribute to various disease conditions, including cognitive disorders, metabolic disorders, and kidney disease (Chan et al., 2016;Chan et al., 2017b;Li et al., 2019a;Li et al., 2019b). Mitochondrial dysfunction can occur as a consequence of the disease, for example in many smoking related diseases, oxidative stress damages mitochondria and results in dysfunction. However, it is now recognized that genetic causes of mitochondrial dysfunction can cause a rare and often inheritable disease called mitochondrial disease, in which patients suffer from fatigue, weakness, and various organ dysfunctions, such as diabetes mellitus and impairment of growth. Mitochondrial disease has a range of severities from relatively mild characterized by unexplained fatigue to severe life limiting disease.

In Chinese Medicine, what is referred to as the kidney is not the same solid organ as the kidney in human anatomy, but is considered as the 'powerhouse' for the whole body as the primary source of energy and heat, regulating multiple functions, including reproduction and development. Interestingly, a condition in Chinese Medicine called 'Kidney Yang' deficiency (KYD) displays some similar symptoms of energy shortage to mitochondrial disease, including fatigue, labor intolerance, cold hypersensitivity (the inability to tolerate cold conditions as a result of the inability to heat the body, especially in the lower limbs), reduced libido and fertility (Zhao et al., 2016); however generally KYD represents mild diseases. The phenotype of KYD also tends to have a familiar heritage, although no specific gene mutation has been reported to date.

Given the role of the mitochondria to produce energy in the form of ATP and produce most of the bodies heat requirements in humans, and fact that mitochondrial disease is inheritable, it has striking similarities to KYD, in that, in KYD the main diagnostic symptoms are "energy shortage" and "cold hypersensitivity" and it is also an inheritable condition. It is therefore a reasonable hypothesis to propose that mitochondrial dysfunction is the key to the development of KYD.

In Chinese Medicine theory, it is believed that prolonged exposure to a cold environment or regular

consumption of cold/frozen food (eg. ice-creams) can lead to KYD (Wang et al., 2006;Dashtdar et al., 2016;Zhu et al., 2018). As such herbal medicines with warm properties are commonly used to treat such conditions (Hempen and Fischer, 2009). It has been shown that prolonged hypothermia may increase oxidative stress, resulting in irreversible impairment in mitochondrial function (Mollica et al., 2005;Hendriks et al., 2019). Furthermore, therapeutic hypothermia has been shown to reduce mitochondrial function (Pamenter et al., 2018). Interestingly in people with mitochondrial diseases, it has been observed that the brain is hypothermic (Rango et al., 2014). If the damaged mitochondria are the result of altered mitochondrial DNA, it is possible that impaired mitochondria would be inherited from the mother to the children.

Previous studies employing the medical examinations for endocrine function found that patients with KYD commonly have reduced urine levels of 17-hydroxycorticosteroids (17-OHCS, a metabolic product of cortisol) with or without reduced serum triiodothyronine (T3) level (Sheng et al., 1979;Shen, 1999;Zhao et al., 2013;Malikov, 2016;Tang et al., 2018). In the clinic, reduced cortisol levels can also contribute to weakness, fatigue, weight loss, and gastrointestinal problems (Adam et al., 2017;Jang et al., 2018). Low serum T3 levels can lead to symptoms like cold sensitivity, edema, weight gain, and muscle weakness (Ruiz-Núñez et al., 2018). However, the clinical features of patients with KYD only have selected symptoms mentioned above and the hormone levels do not warrant replacement therapies, suggesting neither cortisol nor T3 disorders are the primary cause of symptoms in patients with KYD. Other mechanisms are underlying the pathological process of this condition, which are unclear. Understanding such mechanisms can better guide the use of complementary treatment strategies.

The heat generated during ATP synthesis in the mitochondria contributes to core body temperature and muscle shivering is an essential mechanism with exposure to a cold environment (Rajagopal et al., 2019). Mitochondrial number insufficiency and/or dysfunction most likely plays a major role to determine the phenotype of KYD, particularly in thermogenesis tissue BAT and skeletal muscle. Therefore, we hypothesized that the mechanisms underlying the pathophysiology of KYD are due to the dysfunction of mitochondria or a reduced mitochondrial number in the BAT and skeletal muscles. We chose rats with warmth preference as the breeders. Living and working in icy climates can allow the cold to enter the body to quench the 'fire' energy causing Yang deficiency in the kidney, the body's powerhouse (Lyttleton, 2013b). Huang Bai is commonly used in Chinese medicine to correct excess kidney yang energy and overdose can cause the deficiency of yang energy, as KYD. Therefore, both were used in the dams to reinforce the KYD phenotype. We aimed to investigate the changes in body temperature, cold preferences, mitochondrial functional markers, and DNA copy numbers in a rat model of KYD. As mitochondria play a key role in metabolic homeostasis, we also examined lipid

and glucose metabolic profiles in KYD rats. In addition, mitochondrial function is vital for nutrient metabolism (Mollica et al., 2005;Yoon et al., 2010;Miotto et al., 2018). Mitochondrial dysfunction is well known to cause metabolic disorders, such as glucose intolerance (high risk of type 2 diabetes) and dyslipidemia (risk for cardiovascular diseases) (Lionetti et al., 2007;Koves et al., 2008;Yoon et al., 2010;Pinti et al., 2019;You et al., 2020). Therefore, we further hypothesized that rats with KYD phenotype have a higher risk to develop metabolism disorders if a second insult is implemented. To address this hypothesis, we fed the rats with a high-fat diet (HFD) from weaning for 10 weeks and measured their glucose and lipid profile.

2. Methods

2.1 *Animals*

The study was approved by the Animal Ethics Committee of the Chengdu Dossy Experimental Animal Co., Ltd (SCXK (Chuan) 2015-030) where the experiments were performed. A KYD deficiency model was established in both male and female Sprague Dawley rats (10 weeks, Chengdu Dossy Experimental Animal Co., Ltd) according to Chinese Medicine theory. The sires and dams were first screened by the Hot Plate Test. Briefly, rats were allowed to choose to sit/lay on the hot plate set to a temperature of 25ºC or 40ºC for 10 min. In the literature, the preferred temperature for the rat is 24-27ºC (Ray et al., 2004). The percentage of time spent at 40ºC end reflects the preference for hot temperatures. The rats which spent more than 20% of the 10 minutes at 40ºC were selected for further experimentation. The KYD phenotype was further reinforced by cold exposure (ambient temperature 5-8°C, 2h/day) and the supplement of Huang Bai (*Cortex Phellodendri*) in the diet (0.108g/100g chow) in the dams during pregnancy, as previously published (Li et al., 2014). This dose was calculated based on the dose (12g raw herb/day) for human adults according to Chinese Pharmacopoeia and the ratio of body surface area of humans and rats (0.018). Offspring with positive KYD phenotypes from two consecutive generations were kept as KYD rat strain. To validate the relevance of the rat phenotype to human KYD, the offspring were subjected to the Hot Plate Test at 12 weeks of age to evaluate their preference for hot environments. Blood corticosterone and T3 levels were also measured (See the 'Biochemical assays')

2.2 *Experimental study*

At 13 weeks, male offspring were fasted overnight, and the tissues were harvested between 8:00-10:00h. After anesthesia (2% Pentobarbital sodium 40mg/kg), the rectal temperature was measured, followed by cardiac puncture for blood. Blood glucose was immediately measured using a glucose meter (Accu-Check®, Roche Diagnostics, NJ, USA). The plasma was kept at -20°C for hormone and lipid analysis. Brown fat, retroperitoneal white fat, kidney, liver, and skeletal muscle were collected

142   and weighed. Brown fat and skeletal muscle were snap-frozen and kept at -80°C.

143   Considering the vital role of mitochondria in nutrient metabolism, we further examined if the

144   phenotype will increase the risk of metabolic disorders. In a different cohort (n=6), weaning male rat

145   offspring (3 weeks old) were fed a pellet HFD (43% fat, 20kJ/g, Xutong Biological Ltd. Jiangsu,

146   China, following the recipe from our previous studies (Chen et al., 2014;Chen et al., 2018a;Chen et

147   al., 2018b;Komalla et al., 2020)) for 10 weeks. Their littermates were fed the standard rodent chow

148   (14% fat, 12kJ/g). This yielded 4 groups, Control-chow, KYD-chow, Control-HFD, and KYD-HFD.

149   Body weight and food intake were measured every fortnight.

150   **2.3 *Biochemical assays - ELISA***

151   All blood markers were measured by ELISA in plasma using commercially available kits following

152   the manufactures' instructions. Briefly, for the corticosterone assay, plasma was diluted (1:10) before

153   the incubation estimation of levels using the Rat corticosterone ELISA kit, Shanghai Westang

154   Biotechnology, Shanghai, China. The ELISA plate was measured at an OD of 450nm (Synergy H1

155   microplate reader, BioTek, US). For the T3 assay, plasma samples (50ul) were used in the Total T3

156   ELISA assay (IBL International, Hamburg, Germany) and the plate read as above.   LDL

157   measurements were made in plasma samples (5ul). Samples were first incubated with the AAP

158   solution (Shanghai Westang Biotechnology) and the first optical density (OD1) was measured, this

159   was followed by the incubation with enzyme conjugate for the measurement of the second optical

160   density (OD2) at 550nm. The difference between OD2 and OD1 was used to calculate LDL

161   concentration against the standard curve. For cholesterols, plasma samples (20ul) were measured

162   using a kit from Shanghai Westang Biotechnology, the absorbance was measured at 550nm. For

163   insulin, plasma samples were diluted (1:20) and measured using a kit from Crystal Chem, USA, and

164   the absorbance was measured at 450nm.

165   **2.4 *Glucose tolerance test***

166   After 9 weeks of HFD feeding, a glucose tolerance test was carried out in all rats using published

167   methods. After 9 weeks of the diet, the rats were fasted for 5h before an intraperitoneal glucose

168   tolerance test (IPGTT) was performed as previously described (Chen et al., 2014;Chen et al.,

169   2018a;Chen et al., 2018b;Komalla et al., 2020). All mice were administered with D-glucose (2 g/kg,

170   ip). Tail tip blood was collected at time 0 prior to glucose injection (baseline), then at 15, 30, 60, and

171   90 min after glucose administration. Blood glucose levels were measured using a glucose meter

172   (AccuCheck®, Roche Diagnostics). The trapezoid method was used to calculate the area under the

173   curve (AUC) corresponding to the blood glucose levels over the monitoring period obtained for each

174   animal. At 13 weeks, samples were collected following the same protocol as mentioned above.

2.5 *Real-time PCR*

The major function of brown fat is non-shivering thermogenesis against the cold (Cedikova et al., 2016), mainly relying on uncoupling proteins (UCPs), especially UCP1 (Argyropoulos and Harper, 2002). Mice lacking UCPs were cold intolerant (Enerback et al., 1997). Muscle contraction contributes to shivering thermogenesis. mRNA expression of thermoregulator UCP1, mitochondrial biogenesis marker peroxisome proliferator-activated receptor gamma coactivator 1-alpha (PCG1α), and insulin sensing marker Peroxisome proliferator-activated receptor gamma (PPARγ) was measured in brown and skeletal muscle using real-time PCR. Lipid metabolic marker Cholesterol 7 alpha-hydroxylase (CYP7A1) and gluconeogenesis marker Forkhead box protein O (FOXO)1 were measured in the liver. The tissues (10-100mg) were extracted using mirVana™ miRNA Isolation Kit (Life Technologies) following the manufacture's instructions.

Quantification was performed with a two-step reaction process: reverse transcription (RT) and PCR. cDNA was synthesized using HiScript II Q RT SuperMix IIa (Vazyme Biotech Co. Ltd, Jiangsu, China) in a GeneAmp® PCR System 9700 (Applied Biosystems, USA). The genes of interest were measured by SYBR green primers using LightCycler® 480 II Real-time PCR Instrument (Roche, Swiss). The primer sequences were designed in the laboratory and synthesized by Generay Biotech (Generay, China) based on the mRNA sequences obtained from the NCBI database (CYP7A1 5′-CCTGCCGGTACTAGACAGC -3′, reverse 5′- AGGGTCTGGGTAGATTTCAGGA -3′; FOXO1 forward 5′- TAGGAGTTAGTGAGCAGGCAAC -3′, reverse 5′-TGCTGCCAAGTCTGACGAAA-3′; PPARγ forward 5′-ATCAAGAAGACGGAGACAGATA-3′, reverse 5′-GAAGGAACACTTTGTCAGCGA-3′; PGC1-α forward 5′- GGATATACTTTACGCAGGTCG -3′, reverse 5′-ATCGTCTGAGTTTGAATCTAGG-3′; UCP1 forward 5′- TCCGGGCTTAAAGAGCGA -3′, reverse 5′-TGGGTACCGAACTCTCAAC-3′; 18s forward 5′-CGGCTACCACATCCAAGGAA-3′, reverse 5′-GCTGGAATTACCGCGGCT-3′). At the end of the PCR cycles, the melting curve analysis was performed to validate the specific generation of the expected PCR product. mRNA expression was calculated using $2^{-\Delta\Delta Ct}$ methods using 18s as the housekeeping gene. The Control group was assigned the calibrator against which all other results were expressed as fold changes.

The mitochondrial number was measured using the mitochondrial DNA copy number. Genomic DNA was extracted from tissues using the DNeasy Blood and Tissue kit according to the manufacturer's instructions (Qiagen, Hilden, Germany). The content of mtDNA was calculated using real-time quantitative PCR by measuring the threshold cycle ratio (ΔCt) of a mitochondrial-encoded gene (COX1, forward 5′-ACTATACTACTACTAA-CAGACCG-3′, reverse 5′-GGTTCTTTTTTTCCGGAGTA-3′) versus a nuclear-encoded gene (cyclophilin A, forward 5′-

209 ACACGCCATAATGGCACTGG-3′, reverse 5′-CAGTCTTGGCAGTGCAGAT-3′) as we have
210 previously published (Stangenberg et al., 2015).

2.6 *Western blotting*

212 OXPHOS complexes, antioxidant manganese superoxide dismutase (MnSOD), Glutathione
213 peroxidase (GPx), phosphorylated (p)- and total insulin receptor substrate 1 (IRS1) and its
214 downstream protein kinase B (Akt) were measured by Western Blotting. Total and mitochondrial
215 protein was extracted from brown adipose tissue and skeletal muscle using our published method
216 (Chan et al., 2017a). Proteins of the whole tissue lysate and mitochondrial fraction were extracted by
217 the differential speed extraction method. The tissues were homogenized in 200 µl of lysis buffer
218 (Shanghai West Tang Biotechonology Ltd., China). Whole cellular proteins and mitochondria
219 proteins were quantified using Bio-Rad DC protein assay (Bio-Rad Laboratories, California, USA)
220 according to the manufacturer's instructions. Proteins samples (2µg/µl) were loaded into each well
221 of NuPAGE® Novex 4-12% Bis-Tris protein gels (Life Technology, CA, USA) and separated on the
222 gel. The separated proteins were then transferred to PVDF membranes using either semi-dried or wet
223 transfer methods where applies (Thermo Scientific, Illinois, USA). The PVDF membrane was then
224 blocked with 5% skim milk for one hour at room temperature. Primary antibodies (OXPHOS
225 complexes 1:2500, MnSOD 1:5000, GPx-3 1:1000, p-IRS1 1:1000, IRS1 1:1000, p-Akt 1:1000, Akt
226 1:1000, GAPDH 1:1000, Abcam, Cambridge, UK; voltage-dependent anion channels (VDAC)
227 1:1000, Cell signaling technology, MA, USA) were incubated with the PVDF membrane at 4°C
228 overnight, followed by secondary antibodies (peroxidase-conjugated AffiniPure Goat Anti-Rabbit
229 IgG and Peroxidase-conjugated AffiniPure Goat Anti-Mouse IgG, 1:10000, Jackson Immuno
230 Research Laboratories, PA, USA) and SuperSignalTM West Pico Chemiluminescent Substrate
231 (ThermoFisher Scientific, NSW, Australia). The bands on the membrane were detected with LAS-
232 3000 Imaging system (Fujifilm, Tokyo, Japan). The results are expressed as a ratio of the intensity of
233 the protein of interest relative to the band intensity of VDAC for mitochondrial proteins (Wang et al.,
234 2020) or GAPDH for cytoplasmic proteins.

2.7 *Statistical methods*

236 The results are expressed as mean ± SEM. The data between the 2 groups were analyzed by unpaired
237 t-test. The data between the 4 groups were analyzed by two-way ANOVA followed by post hoc
238 Fisher's LSD tests. The data of IPGTT were analyzed by ANOVA with repeated measures followed
239 by Fisher's LSD tests. Prism V9.0.1 (GraphPad Software, CA, USA) and Statistica (StatSoft, TIBCO
240 Software, CA, USA) were used for data analysis. $P<0.05$ was considered statistically significant.

3. Results

3.1 Baseline assessment in the KYD rats

3.1.1 *Biometric parameters*

Before pregnancy, KYD dams were 9% smaller than the controls (P<0.05), consistent with weight loss in patients with KYD (Lyttleton, 2013b). The litter size of KYD mothers (6.33 ± 0.88) was also half of the Control group (13 ± 1.16, P<0.05). KYD dams seem to produce less female offspring in each litter reflected by the sex ratio (female to male: KYD 1.57 ± 0.81, Control 2.37 ± 1.20). However, it did not have statistical significance. Thus, KYD dams showed issues of reproduction.

Male offspring from KYD dams had significantly smaller birth weight (P<0.01 vs Control, Figure 1a), which was maintained in adulthood (P<0.05 vs Control, Table 1). KYD offspring also had smaller kidney mass (P<0.05 vs Control) and white fat mass (P<0.01 vs Control), however bigger muscle mass at 13 weeks (P< 0.05 vs Control, Table 1). After standardizing for body weight, KDY rats had a bigger percentage of liver and muscle weights (both P< 0.05 vs Control), and a smaller percentage of white fat mass (P<0.01, Table 1).

3.1.2 *Serum metabolic markers*

To further confirm the human relevance of this rat model, we measured serum corticosterone and T3 levels. In KYD offspring, serum corticosterone levels were significantly lower than the Control group (P<0.05, Table 1), while T3 levels were only marginally reduced (Table 1).

We also measured blood glucose and lipid levels. The blood glucose level in the KYD offspring was similar to the Control group (Table 1), whereas serum LDL and cholesterol levels were significantly increased in KYD offspring (P< 0.05 and 0.01 vs Control, respectively, Table 1), suggesting lipid metabolic disorders, which is also consistent with the risk in human patients.

3.1.3 *Body temperature and warm/cold preference*

The hot plate test allows the rats to choose their preferred temperature by sitting or laying or either of two plates set to temperatures of 25ºC as cool and 40ºC as warm. KYD rats showed a preference for warm locations which was reflected in the rats spending twice as long as the Control rats on the warm plate (P<0.05 vs Control, Figure 1a), showing a preference for warm locations.

To investigate whether such preference was due to low core body temperature, we measured rectal temperature and mRNA expression of uncoupling proteins (UCP)1 in BAT (non-shivering thermogenesis) and muscle (shivering thermogenesis). However, there was no difference in body temperature between the KDY offspring and Control offspring (Figure 1b). Not surprisingly, the regulator of thermogenesis UCP1 expression was not significantly changed in both BAT and skeletal muscle (Figure 1c,d).

3.1.4 *Mitochondrial metabolic markers in the BAT and muscle*

In BAT, ATP production was significantly lower in the KYD rats (P< 0.01 vs Control, Figure 2a). Peroxisome proliferator-activated receptor gamma coactivator 1-alpha (PGC1a) is a multiple-functional molecule, which also regulates mitochondrial biogenesis. PCG1α in BAT was reduced in KYD rats (P<0.05, vs Control, Figure 2b), suggesting impaired ability to replenish mitochondrial shortage. This is associated with reduced mitoDNA copy number (P< 0.001 vs Control, Figure 2c). Results show that OXPHOS CI was nearly diminished in KYD rats, and OXPHOS CV was also significantly lower in KYD rats (both P<0.05 vs Control, Figure 2d,e). Endogenous antioxidants MnSOD and GPx were not different between the groups (data not shown), suggesting oxidative stress is not involved.

In the skeletal muscle, ATP levels were significantly higher in the KYD rats (P<0.05 vs Control, Figure 3a). Mitochondrial biogenesis and metabolic regulator PCG1α was lower in the KYD rats (P=0.07 vs Control, Figure 3b), however mitochondrial DNA copy number was not different between the groups (Figure 3c), suggesting impaired metabolic capacity in the muscle. OXPHOS CI was not different between the groups (Figure 3d), however, OXPHOS CV was nearly depleted in the skeletal muscle (P < 0.01, Figure 3e). Similarly, in BAT, mitochondrial endogenous antioxidant MnSOD and GPx did not show any difference between the Control and KYD groups (not shown). Therefore, the difference between mitochondrial biogenesis and functional units might not result from oxidative stress.

3.2 Effects of HFD consumption on metabolic profiles

At weaning, the body weights were not significantly different among the groups (Table 2). At 13 weeks, KYD-chow rats were smaller than the Control-chow rats (P<0.05, Table 2), consistent with the first cohort. Interestingly, KYD-HFD rats gained less body weight by HFD consumption compared with the Control rats (P<0.01 KYD-HFD vs Control-HFD, Table 2) whose body weight was similar to the Control-chow rats, although KYD rats had similar daily caloric intake as the Control regardless of the diet (Table 2). HFD consumption significantly increased white fat mass in both Control-HFD and KYD-HFD rats (P < 0.05, Table 2), but only increased liver mass in the KYD-HFD rats (P < 0.01 vs KYD-chow, Table 2) both as net weight and percentage of body weight.

During the glucose tolerance test, it was expected that Control-HFD rats developed glucose intolerance reflected by higher blood glucose levels at 30 min post glucose injection (P<0.01, Figure 4a) and bigger AUC value (P<0.01 vs Control-chow, Figure 4b); however, KYD-HFD rats showed more severe glucose intolerance than Control HFD rats as shown by blood glucose level at 15 min and 30 min post glucose injection (Figure 4a) and AUC value (P<0.01 KYD-HFD vs KYD-chow and Control-HFD, Figure 4b) albeit smaller body weight and fat mass. This may be due to insulin

insufficiency, as serum insulin level (P<0.01 Control-HFD vs Control-chow and KYD-HFD) was significantly increased in the Control-HFD group, but remained unchanged in the KYD-HFD rats. Interestingly, hyperlipidemia was worsened in KYD rats after HFD consumption, especially the LDL which was increased in the KYD-HFD group (P<0.01 KYD-HFD vs KYD-chow and Control-HFD, Table 2), not the Control-HFD group. Cholesterol was increased in Control-HFD group (P<0.05 vs Control-chow Table 2), which was further increased in the KYD-HFD group (P<0.05 vs Control-HFD, P<0.01 vs KYD-chow group, Table 2)

To further investigate the molecular pathway, we found in the muscle, the energy regulator PGC-1α was significantly downregulated in the KYD-chow rats (P<0.05 vs Control-chow, Figure 4c), which was less reduced in the Control-HFD and KYD-HFD rats, suggesting diet and phenotype may independently affect this marker. The insulin sensing marker PPARγ expression was only reduced by HFD consumption (P<0.01 Control-HFD vs Control-chow, KYD-HFD vs KYD-chow, Figure 4d). The ratio between p-IRS1 and total IRS1 was reduced in KYD-chow rats and by HFD consumption (both P<0.01, Figure 4e). However, there was some increase in p-IRS1/IRS1 in KYD-HFD rats compared with their chow-fed littermates (P<0.01). The downstream signaling p-Akt/Akt ratio was only reduced in KYD rats independent of the diet (P<0.01 vs Control rats fed the same diet, Figure 4f). In the liver, FOXO1 expression was suppressed in the KYD-chow rats (P<0.01 vs Control-chow, Figure 4g), and to a less extent in the Control-HFD-rats (P<0.01 vs Control-chow); however, FOXO1 was significantly upregulated by HFD feeding in KYD rats (P<0.05 KYD-HFD cs KYD-chow, Figure 4g). The lipid metabolic marker CYP7A1 was more than halved in the liver of the KYD-rats albeit without statistical significance (Figure 4h). CYP7A1 mRNA was however increased in Control-HFD (P<0.01 vs Control-chow), which was at a normal level in KYD-HFD rats (P<0.01 vs Control-HFD).

4. Discussion

As the kidney in Chinese Medicine is considered the 'powerhouse', the condition of KYD is mostly caused by mitochondrial dysfunction. In this study, we used a clinically relevant rat model to demonstrate that in KYD, markers of the mitochondrial number, biogenesis, and function are differentially regulated in different key heat production organs, which may contribute to the warm preference but unchanged core body temperature. Reduced metabolic main regulator PCG1α may contribute to blood hyperlipidemia.

The KYD rats showed a similar phenotype as the humans with KYD (Sheng et al., 1979;Shen, 1999;Lyttleton, 2013b;a;Zhao et al., 2013;Malikov, 2016;Tang et al., 2018), including warm preference, issues of reproduction small birth weight, slow postnatal growth, impaired fertility

function, hyperlipidemia, and reduced corticosterone levels, suggesting its clinical relevance. According to the theory of Chinese medicine, KYD is closely related to lifestyle or environment, such as living and working in icy climates (Lyttleton, 2013b). However, the dietary supplement Huang Bai is not known to suppress T3, rather its anti-inflammatory and gonadotropin-releasing hormone suppressing effects (Xian et al., 2011;Lee et al., 2016;Sun et al., 2019). This is may explain reduced corticosterone levels, which is also anti-inflammatory hormone. However, reduced T3 levels in some patients with KYD may be secondary to reduced energy supply, which is not seen in this rat model.

As the cellular powerhouse in modern science, electron respiration within the mitochondrial OXPHOS complex generate both ATP to fuel the cells, and heat to warm the body. In small rodents and infants, BAT is a discrete organ for heat production; whereas in adult humans, brown adipocytes diffuse into white fat tissue, skeletal muscles, and around major arteries to maintain core temperature (Ravussin and Galgani, 2011). Here in the KYD rats, ATP production is significantly reduced in BAT, and somehow it was partially compensated by muscle ATP production. In Chinese medicine, Kidney-yang is the source of energy to promote blood movement. Therefore KYD can affect microcirculation in the limbs resulting in cold extremities (Shu et al., 2000). In humans, cold intolerance in KYD patients mainly occurs in the low limbs and not in the whole body, which may explain why KYD rats prefer warm places although the core body temperature did not change.

ATP reduction in BAT may directly attribute to reduced mitochondrial number and biogenesis, reflected by mitoDNA number and PCG1α expression, respectively. In addition, OXPHOS complexes, where electron enters the inner membrane OXPHOS CI and ATP is produced in OXPHOS CV, were both reduced contributing to reduced ATP production. In the muscle, we observed significantly increased ATP production. However, although the mitochondrial number and OXPHOS CI seem to be unchanged, OXPHOS CV was depressed in the muscle. It is unclear whether this is an outcome of the overproduction of ATP, or it is an outcome of KYD, which requires further investigation. Reactive oxygen species (ROS) are released as a by-product during ATP production, which is normally consumed by endogenous antioxidants, such as MnSOD and GPx. Thus if MnSOD and GPx are overconsumed, increased oxidative stress can damage the mitochondria and cells. Mitochondrial antioxidant MnSOD and GPx did not show any difference between the Control and KYD groups in both BAT and muscle. Therefore, the differences between mitochondrial biogenesis and functional units are unlikely to be due to oxidative stress.

Mitochondria have been implicated as key factors regulating reproductive processes (Kumar and Sangeetha, 2009;Cecchino et al., 2018). The downregulation of mitochondrial biogenesis marker PGC1α and OXPHOS CV may play some role in reduced litter size in KYD dams. In addition, the healthy mitochondrial function also plays a key role in maintaining nutrient homeostasis, and is the

main regulator for both glucose and lipid metabolism (Gerhart-Hines et al., 2007;Handschin et al., 2007). However, reduced PGC1α seems to only affect the blood lipid profile, maybe because of the need for glucose being used to produce ATP in the muscle. Therefore, we postulate that mitochondrial insufficiency and dysfunction is the underlying mechanism of hyperlipidemia observed in patients with KYD (Zhang et al., 1989;Liu and Shan, 2017).

The highlight of this study is the introduction of a second insult, *ad libitum* HFD feeding, which confirmed our hypothesis that KYD rats are prone to glucose and lipid metabolic disorders when the obesogenic environment is present. KYD and control rats had similar body weights at weaning. We think the recovery of body weight at weaning is related to breastmilk, which is full of antioxidants and nutrients. Thus, breastfeeding may promote catch growth in rats with in-utero underdevelopment. After weaning, the loss of protection from breastmilk and dysfunctional mitochondrial function resulted in retarded growth in KYD rats after weaning. However, KYD rats did not gain as much weight as the Control rats, yet exhibit more severe glucose and lipid disorders, suggesting underlying dysfunction in tissue nutrient metabolism. The unchanged serum insulin in the KYD-HFD group, suggesting the inability of the pancreas to produce more insulin in response to increased energy influx, eg. rising in blood glucose level after meals. Muscle is a major organ for insulin-stimulated glucose deposition. Therefore, we investigated markers related to glucose metabolism in the muscle. Previously, we have found that in rats with glucose intolerance, PGC1a is the main switch for energy sensing and metabolism. Its expression is significantly reduced in skeletal muscle (Simar et al., 2011;Chan et al., 2015), which was only displayed in KYD-chow rats, whereas there was only a marginal reduction in Control-HFD rats. The change in KYD-chow rats may already determine their poor metabolic capability. Insulin sensing marker PPARγ was suppressed by HFD consumption in both HFD and KYD-HFD rats, which can only explain increased insulin resistance by HFD consumption, which can't explain why KYD-HFD had more severe glucose intolerance. Then, we further investigated the liver, which plays a key role in both glucose homeostasis and lipid metabolism (especially in the synthesis of cholesterol and major lipoproteins, eg. LDL). What needs to be noted here is the increased gluconeogenesis marker FOXO1 in KYD-HFD rats compared with their chow-fed littermates. Although the level is comparable to a normal level as reflected in the Control-chow rats, such an increase is perhaps sufficient to cause higher blood glucose levels during glucose tolerance test thereafter more severe glucose intolerance in KYD-HFD rats compared with Control-HFD rats, whose FOXO1 was actually suppressed by HFD feeding.

Another worsened profile in KYD-HFD rats is the blood lipids, ie. LDL and cholesterol. CYP7A1 is an important enzyme to regulate cholesterol metabolism. In humans, CYP7A1 deficiency is directly related to increased circulating cholesterol and LDL levels (Pullinger et al., 2002). Overexpression

of CYP7A1 in the liver can protect against HFD-induced obesity (Li et al., 2010). Here, we observed a marked increase in this enzyme in HFD-fed mice, which may be an adaptive change to prevent further increase in circulating cholesterol and LDL levels. Interestingly, such adaptation was lost in KYD rats when they consumed the HFD diet, attribute to its low baseline level in the KYD-chow rats. As such, dyslipidemia seems more problematic in KYD-HFD rats. Future studies can follow up on the cardiovascular consequence in these rats.

We need to acknowledge the limitation of using rats to model a condition with no clear origins, which represents a partial match to the phenotype of human patients. However, it may still be useful to determine the risk of other conditions, such as vascular damage, and investigate the efficacy of certain treatments to improve mitochondrial function.

5. Conclusion

The 'kidney yang' in Chinese Medicine seems to be closely related to abnormal mitochondrial function. This study showed abnormal mitochondrial functional units in both BAT and skeletal muscle with impaired ATP production in BAT. There seems to be an adaptive increase in muscle ATP production, KYD rats still showed abnormal temperature sensation and hyperlipidemia, suggesting impaired mitochondrial metabolic function (summarized in Figure 5). This may contribute to exacerbated glucose and lipid metabolic disorders when HFD was introduced in KYD rats.

6. Conflict of interests

The authors declare that they have no competing interests.

7. Author's contribution

YC, BGO, and HChen designed the study. HCai and HL performed the animal studies and collected the tissues. Hcai, XH, JE, YS, WL analyzed the tissues. HChen drafted the manuscript. All authors contributed to the final manuscript and approved the submission.

8. Funding

439   University Key Training Program for Youth Teachers (F7201931620002).

9. Acknowledgment

441   NA

10. References

Adam, E.K., Quinn, M.E., Tavernier, R., Mcquillan, M.T., Dahlke, K.A., and Gilbert, K.E. (2017). Diurnal cortisol slopes and mental and physical health outcomes: A systematic review and meta-analysis. *Psychoneuroendocrinology* 83**,** 25-41.

Argyropoulos, G., and Harper, M.E. (2002). Uncoupling proteins and thermoregulation. *J Appl Physiol* 92**,** 2187-2198.

Cecchino, G.N., Seli, E., Alves Da Motta, E.L., and García-Velasco, J.A. (2018). The role of mitochondrial activity in female fertility and assisted reproductive technologies: overview and current insights. *Reproductive BioMedicine Online* 36**,** 686-697.

Cedikova, M., Kripnerová, M., Dvorakova, J., Pitule, P., Grundmanova, M., Babuska, V., Mullerova, D., and Kuncova, J. (2016). Mitochondria in White, Brown, and Beige Adipocytes. *Stem Cells International* 2016**,** 6067349.

Chan, Y.L., Oliver, B.G., and Chen, H. (2020). What lessons have we learnt about the impact of maternal cigarette smoking from animal models? *Clinical and Experimental Pharmacology and Physiology* 47**,** 337-344.

Chan, Y.L., Saad, S., Al-Odat, I., Oliver, B., Pollock, C., M. Jones, N., and Chen, H. (2017a). Maternal L-Carnitine supplementation improves brain health in offspring from cigarette smoke exposed mothers. *Frontiers in Molecular Neuroscience* 10**,** 33.

Chan, Y.L., Saad, S., Machaalani, R., Oliver, B.G., Vissel, B., Pollock, C., Jones, N.M., and Chen, H. (2017b). Maternal Cigarette Smoke Exposure Worsens Neurological Outcomes in Adolescent Offspring with Hypoxic-Ischemic Injury. *Frontiers in Molecular Neuroscience* 10**,** 306.

Chan, Y.L., Saad, S., Pollock, C., Oliver, B., Al-Odat, I., Zaky, A.A., Jones, N., and Chen, H. (2016). Impact of maternal cigarette smoke exposure on brain inflammation and oxidative stress in male mice offspring. *Sci Rep* 6**,** 25881.

Chan, Y.L., Saad, S., Simar, D., Oliver, B., Mcgrath, K., Reyk, D.V., Bertrand, P.P., Gorrie, C., Pollock, C., and Chen, H. (2015). Short term exendin-4 treatment reduces markers of metabolic disorders in female offspring of obese rat dams. *International Journal of Developmental Neuroscience* 46**,** 67-75.

Chen, H., Ng, J.P.M., Bishop, D.P., Milthorpe, B.K., and Valenzuela, S.M. (2018a). Gold nanoparticles as cell regulators: beneficial effects of gold nanoparticles on the metabolic profile of mice with pre-existing obesity. *Journal of Nanobiotechnology* 16**,** 88.

Chen, H., Ng, J.P.M., Tan, Y., Mcgrath, K., Bishop, D.P., Oliver, B., Chan, Y.L., Cortie, M.B., Milthorpe, B.K., and Valenzuela, S.M. (2018b). Gold nanoparticles improve metabolic profile of mice fed a high-fat diet. *Journal of Nanobiotechnology* 16**,** 11.

Chen, H., Simar, D., Pegg, K., Saad, S., Palmer, C., and Morris, M. (2014). Exendin-4 is effective against metabolic disorders induced by intrauterine and postnatal overnutrition in rodents. *Diabetologia* 57**,** 614-622.

Dashtdar, M., Dashtdar, M.R., Dashtdar, B., Kardi, K., and Shirazi, M.K. (2016). The Concept of Wind in Traditional Chinese Medicine. *Journal of pharmacopuncture* 19**,** 293-302.

Dudkina, N.V., Kouřil, R., Peters, K., Braun, H.-P., and Boekema, E.J. (2010). Structure and function of mitochondrial supercomplexes. *Biochimica et Biophysica Acta (BBA) - Bioenergetics* 1797**,** 664-670.

Enerback, S., Jacobsson, A., Simpson, E.M., Guerra, C., Yamashita, H., Harper, M.-E., and Kozak,

L.P. (1997). Mice lacking mitochondrial uncoupling protein are cold-sensitive but not obese. *Nature* 387, 90-94.

Gerhart-Hines, Z., Rodgers, J.T., Bare, O., Lerin, C., Kim, S.H., Mostoslavsky, R., Alt, F.W., Wu, Z., and Puigserver, P. (2007). Metabolic control of muscle mitochondrial function and fatty acid oxidation through SIRT1/PGC-1alpha. *EMBO J* 26, 1913-1923.

Handschin, C., Choi, C.S., Chin, S., Kim, S., Kawamori, D., Kurpad, A.J., Neubauer, N., Hu, J., Mootha, V.K., Kim, Y.-B., Kulkarni, R.N., Shulman, G.I., and Spiegelman, B.M. (2007). Abnormal glucose homeostasis in skeletal muscle specific PGC-1alpha knockout mice reveals skeletal muscle pancreatic b cell crosstalk. *J Clin Invest* 117, 3463-3474.

Hempen, C.-H., and Fischer, T. (2009). "IX - Herbs that warm the interior and expel cold," in *A Materia Medica for Chinese Medicine,* eds. C.-H. Hempen & T. Fischer. (Edinburgh: Churchill Livingstone), 381-411.

Hendriks, K.D.W., Brüggenwirth, I.M.A., Maassen, H., Gerding, A., Bakker, B., Porte, R.J., Henning, R.H., and Leuvenink, H.G.D. (2019). Renal temperature reduction progressively favors mitochondrial ROS production over respiration in hypothermic kidney preservation. *Journal of Translational Medicine* 17, 265.

Jang, Y., Kim, J.H., Lee, H., Lee, K., and Ahn, S.H. (2018). A quantile regression approach to explain the relationship of Fatigue and Cortisol, Cytokine among Koreans with Hepatitis B. *Scientific reports* 8, 16434-16434.

Komalla, V., Sheikholeslami, B., Li, G., Bokshi, B., Chan, Y.L., Ung, A., Gregory Oliver, B., Chen, H., and Haghi, M. (2020). Impact of A Cargo-Less Liposomal Formulation on Dietary Obesity-Related Metabolic Disorders in Mice. *Int J Mol Sci* 21.

Koves, T.R., Ussher, J.R., Noland, R.C., Slentz, D., Mosedale, M., Ilkayeva, O., Bain, J., Stevens, R., Dyck, J.R.B., Newgard, C.B., Lopaschuk, G.D., and Muoio, D.M. (2008). Mitochondrial overload and incomplete fatty acid oxidation contribute to skeletal muscle insulin resistance. *Cell Metabolism* 7, 45-56.

Kumar, D.P., and Sangeetha, N. (2009). Mitochondrial DNA mutations and male infertility. *Indian journal of human genetics* 15, 93-97.

Lee, S.H., Kwak, S.C., Kim, D.K., Park, S.W., Kim, H.S., Kim, Y.-S., Lee, D., Lee, J.W., Lee, C.G., Lee, H.K., Cho, S.-M., Shin, Y.J., Lee, J.Y., Kim, H., and Chang, G.T. (2016). Effects of Huang Bai (Phellodendri Cortex) and Three Other Herbs on GnRH and GH Levels in GT1-7 and GH3 Cells. *Evidence-based complementary and alternative medicine : eCAM* 2016, 9389028-9389028.

Li, G., Chan, Y.L., Nguyen, L.T., Mak, C., Zaky, A., Anwer, A.G., Shi, Y., Nguyen, T., Pollock, C.A., Oliver, B.G., Saad, S., and Chen, H. (2019a). Impact of maternal e-cigarette vapor exposure on renal health in the offspring. *Annals of the New York Academy of Sciences* 1452, 65-77.

Li, G., Chan, Y.L., Sukjamnong, S., Anwer, A.G., Vindin, H., Padula, M., Zakarya, R., George, J., Oliver, B.G., Saad, S., and Chen, H. (2019b). A Mitochondrial Specific Antioxidant Reverses Metabolic Dysfunction and Fatty Liver Induced by Maternal Cigarette Smoke in Mice. *Nutrients* 11, 1669.

Li, T., Owsley, E., Matozel, M., Hsu, P., Novak, C.M., and Chiang, J.Y. (2010). Transgenic expression of cholesterol 7alpha-hydroxylase in the liver prevents high-fat diet-induced obesity and insulin resistance in mice. *Hepatology* 52, 678-690.

Li, W.-H., Li, Q.-J., Li, W.-Z., Liu, W.-W., Zeng, Y.-Z., Zhang, T.-E., Zhang, X.-G., Sun, S.-Q., Wang, M.-Q., and Ding, W.-J. (2014). The Fourier transform infrared spectra of the key organs derived from Kidney (Shen)-yang deficiency syndrome mice. *Chinese Journal of Integrative Medicine* 20, 829-834.

Lionetti, L., Mollica, M.P., Crescenzo, R., D'andrea, E., Ferraro, M., Bianco, F., Liverini, G., and Iossa, S. (2007). Skeletal muscle subsarcolemmal mitochondrial dysfunction in high-fat fed rats exhibiting impaired glucose homeostasis. *Int J Obes* 31, 1596-1604.

Liu, F., and Shan, L. (2017). An exploration on TCM syndrome differentiation rules and clinical

538   syndromes distribution of hyperlipidemia. *Clinical Journal of Chinese Medicine* 9**,** 47-48.

539 Lyttleton, J. (2013a). "4 - Diagnosis and Treatment of Female Infertility," in *Treatment of Infertility*
540   *with Chinese Medicine (Second Edition),* ed. J. Lyttleton. Churchill Livingstone), 66-139.

541 Lyttleton, J. (2013b). "12 - Diet and lifestyle," in *Treatment of Infertility with Chinese Medicine*
542   *(Second Edition),* ed. J. Lyttleton. Churchill Livingstone), 406-440.

543 Malikov, D. (2016). Traditional Chinese Medicine Approach to Hypothyroidism *International*
544   *Journal of Complementary & Alternative Medicine* 5**,** 00142.

545 Miotto, P.M., Mcglory, C., Holloway, T.M., Phillips, S.M., and Holloway, G.P. (2018). Sex-
546   differences in mitochondrial respiratory function in human skeletal muscle. *American*
547   *Journal of Physiology-Regulatory, Integrative and Comparative Physiology* 0**,** null.

548 Mollica, M.P., Lionetti, L., Crescenzo, R., Tasso, R., Barletta, A., Liverini, G., and Iossa, S. (2005).
549   Cold exposure differently influences mitochondrial energy efficiency in rat liver and skeletal
550   muscle. *FEBS Letters* 579**,** 1978-1982.

551 Pamenter, M.E., Lau, G.Y., and Richards, J.G. (2018). Effects of cold on murine brain
552   mitochondrial function. *PLOS ONE* 13**,** e0208453.

553 Pinti, M.V., Fink, G.K., Hathaway, Q.A., Durr, A.J., Kunovac, A., and Hollander, J.M. (2019).
554   Mitochondrial dysfunction in type 2 diabetes mellitus: an organ-based analysis. *American*
555   *Journal of Physiology-Endocrinology and Metabolism* 316**,** E268-E285.

556 Pullinger, C.R., Eng, C., Salen, G., Shefer, S., Batta, A.K., Erickson, S.K., Verhagen, A., Rivera,
557   C.R., Mulvihill, S.J., Malloy, M.J., and Kane, J.P. (2002). Human cholesterol 7alpha-
558   hydroxylase (CYP7A1) deficiency has a hypercholesterolemic phenotype. *The Journal of*
559   *clinical investigation* 110**,** 109-117.

560 Rajagopal, M.C., Brown, J.W., Gelda, D., Valavala, K.V., Wang, H., Llano, D.A., Gillette, R., and
561   Sinha, S. (2019). Transient heat release during induced mitochondrial proton uncoupling.
562   *Communications Biology* 2**,** 279.

563 Rango, M., Arighi, A., Bonifati, C., Del Bo, R., Comi, G., and Bresolin, N. (2014). The brain is
564   hypothermic in patients with mitochondrial diseases. *J Cereb Blood Flow Metab* 34**,** 915-
565   920.

566 Ravussin, E., and Galgani, J.E. (2011). The implication of brown adipose tissue for humans. *Annual*
567   *review of nutrition* 31**,** 33-47.

568 Ray, B., Mallick, H.N., and Kumar, V.M. (2004). Changes in thermal preference, sleep–
569   wakefulness, body temperature and locomotor activity of rats during continuous recording
570   for 24 hours. *Behavioural Brain Research* 154**,** 519-526.

571 Ruiz-Núñez, B., Tarasse, R., Vogelaar, E.F., Janneke Dijck-Brouwer, D.A., and Muskiet, F.a.J.
572   (2018). Higher Prevalence of "Low T3 Syndrome" in Patients With Chronic Fatigue
573   Syndrome: A Case-Control Study. *Frontiers in endocrinology* 9**,** 97-97.

574 Shen, Z. (1999). The location of deficiency syndrome of kidney Yang. *Chinese medical journal*
575   112**,** 973-975.

576 Sheng, Z., Zhang, L., Zha, L., Shi, S., and Gu, T. (1979). The pituitary gland in patients with kidney
577   yang deficiency - the changes in Adrenal cortex system. *Shanghai Journal of Traditional*
578   *Chinese Medicine* 2**,** 34-37.

579 Shu, Y., Jia, J., Xu, X., and Want, Z. (2000). Observation on pulse hemodynamics in 57 patients
580   with kidney deficiency. *Inner Mongolia Chinese Medicine* 4**,** 5-6.

581 Simar, D., Chen, H., Lambert, K., Mercier, J., and Morris, M.J. (2011). Interaction between
582   maternal obesity and post-natal over-nutrition on skeletal muscle metabolism. *Nutr Metab*
583   *Cardiovasc Dis* 22**,** 269-276.

584 Stangenberg, S., Nguyen, L.T., Chen, H., Al-Odat, I., Killingsworth, M.C., Gosnell, M.E., Anwer,
585   A.G., Goldys, E.M., Pollock, C.A., and Saad, S. (2015). Oxidative stress, mitochondrial
586   perturbations and fetal programming of renal disease induced by maternal smoking. *Int J*
587   *Biochem Cell Biol* 64**,** 81-90.

588 Sun, Y., Lenon, G.B., and Yang, A.W.H. (2019). Phellodendri Cortex: A Phytochemical,
589   Pharmacological, and Pharmacokinetic Review. *Evidence-based complementary and*

alternative medicine : eCAM 2019**,** 7621929-7621929.

Tang, N., Liu, L., Qiu, H., Shi, W., and Mao, D. (2018). Analysis of gene expression and functional changes of adrenal gland in a rat model of kidney yang deficiency syndrome treated with Sini decoction. *Experimental and therapeutic medicine* 16**,** 3107-3115.

Wang, J., Zhu, P., Li, R., Ren, J., and Zhou, H. (2020). Fundc1-dependent mitophagy is obligatory to ischemic preconditioning-conferred renoprotection in ischemic AKI via suppression of Drp1-mediated mitochondrial fission. *Redox biology* 30**,** 101415-101415.

Wang, J.G., Pan, L., Wu, B., and Wang, M. (2006). Familial Characteristics of Kidney-Yang Deficiency and Cold Syndrome. *Journal of Toxicology and Environmental Health, Part A* 69**,** 1939-1950.

Xian, Y.-F., Mao, Q.-Q., Ip, S.-P., Lin, Z.-X., and Che, C.-T. (2011). Comparison on the anti-inflammatory effect of Cortex Phellodendri Chinensis and Cortex Phellodendri Amurensis in 12-O-tetradecanoyl-phorbol-13-acetate-induced ear edema in mice. *Journal of Ethnopharmacology* 137**,** 1425-1430.

Yoon, J.C., Ng, A., Kim, B.H., Bianco, A., Xavier, R.J., and Elledge, S.J. (2010). Wnt signaling regulates mitochondrial physiology and insulin sensitivity. *Genes & development* 24**,** 1507-1518.

You, B., Dun, Y., Zhang, W., Jiang, L., Li, H., Xie, M., Liu, Y., and Liu, S. (2020). Anti-insulin resistance effects of salidroside through mitochondrial quality control. *J Endocrinol* 244**,** 383.

Zhang, W., Wang, W., Shi, T., Zhou, W., Wang, J., Wang, Z., Liu, H., Zhao, D., and Chen, K. (1989). Changes of plasma lipid peroxide, high-density lipoprotein cholesterol, and its subcomponent levels in elderly patients with kidney deficiency. *Chinese Medicine Journal* 2**,** 43-46.

Zhao, L., Wu, H., Qiu, M., Sun, W., Wei, R., Zheng, X., Yang, Y., Xin, X., Zou, H., Chen, T., Liu, J., Lu, L., Su, J., Ma, C., Zhao, A., and Jia, W. (2013). Metabolic Signatures of Kidney Yang Deficiency Syndrome and Protective Effects of Two Herbal Extracts in Rats Using GC/TOF MS. *Evid Based Complement Alternat Med* 2013**,** 540957.

Zhao, T., Wang, H., Yu, C., Wang, J., Cui, Y., Zheng, X., Wang, B., Wang, W., and Meng, J. (2016). Classification and differentiation between kidney yang and yin decficiency syndromes in TCM based on decision tree analysis method. *Int J Clin Exp Med* 9**,** 21888-21899.

Zhu, J., Liu, S., Guo, Y., Hou, L., Su, X., Li, Y., Han, B., Liu, D., Wang, Q., Chen, J.J.D., and Wei, W. (2018). A New Model of Diarrhea with Spleen-Kidney Yang Deficiency Syndrome. *Evidence-Based Complementary and Alternative Medicine* 2018**,** 4280343.

Table 1: Biometric parameters and blood metabolic markers in male offspring at 13 weeks.

	Control	KYD
Birth weight at birth (g)	7.80 ± 0.20	4.78 ± 0.29**
Body weight at 13 weeks (g)	322 ± 70	286 ± 96*
Liver (g)	10.28±0.24	10.68±0.21
Liver %	2.88±0.06	3.32±0.13*
Kidney (g)	2.46±0.10	2.06±0.06*
Kidney %	0.71±0.02	0.64±0.03
Brown adipose tissue (g)	0.50±0.05	0.47±0.05
Brown adipose tissue %	0.14±0.01	0.15±0.02
White adipose tissue (g)	4.96±0.32	2.80±0.31**
White adipose tissue%	1.39±0.09	0.86±0.08**
Sketeal muscle (g)	0.53±0.04	0.69±0.04*
Sketeal muscle %	0.15±0.01	0.22±0.02*
Serum corticosterone (ng/ml)	22.2 ± 0.8	15.2 ± 1.4*
Serum T3 (ng/ml)	3.84 ± 0.15	3.68 ± 0.11
Blood glucose (mM)	8.05 ± 0.37	7.83 ± 0.51
Serum LDL (mM)	1.11 ± 0.06	1.26 ± 0.03*
Serum Cholesterol (mM)	2.21 ± 0.08	2.76 ± 0.12**

Results are expressed as mean ± SEM, n=10. * P < 0.05, ** P< 0.01.

LDL: Low-Density Lipoprotein; T3: triiodothyronine.

Table 2: Biometric parameters and blood metabolic markers in male offspring fed a HFD.

|	Control-chow	KYD-chow	Control-HFD	KYD-HFD
Body weight before the diet (g)	53.0 ± 0.5	50.8 ± 1.4	52.0 ± 1.3	53.0 ± 0.7
Body weight at endpoint (g)	375 ± 9	323 ± 15*	442 ± 12**	380 ± 9$^{\#\#\delta}$
Caloric intake (kJ/day/rat)	271 ± 16	275 ± 14	348 ± 12*	403 ± 35 $^{\delta\delta}$
Liver (g)	11.4 ± 0.5	10.7 ± 0.75	13.7 ± 0.9	14.2 ± 0.7 $^{\delta\delta}$
Liver %	2.97 ± 0.20	3.01 ± 0.07	3.16 ± 0.15	3.71 ± 0.09 $^{\delta\delta}$
White adipose tissue (g)	4.99 ± 0.82	3.56 ± 0.48	9.76 ± 1.71 *	8.47 ± 0.90 $^{\delta}$
White adipose tissue%	1.28 ± 0.20	0.89 ± 0.07	1.88 ± 0.22 *	2.20 ± 0.20 $^{\delta\delta}$
Sketeal muscle (g)	0.71 ± 0.04	0.74 ± 0.05	0.82 ± 0.03	0.78 ± 0.02
Sketeal muscle %	0.18 ± 0.01	0.19 ± 0.00	0.20 ± 0.01	0.20 ± 0.01
Blood insulin (ng/ml)	0.15 ± 0.03	0.12 ± 0.01	0.29 ± 0.05**	0.15 ± 0.03$^{\#\#}$
Serum LDL (mM)	1.20 ± 0.07	1.41 ± 0.05*	1.49 ± 0.08**	2.01 ± 0.08$^{\#\#\delta\delta}$
Serum Cholesterol (mM)	2.51 ± 0.05	2.71 ± 0.08	3.00 ± 0.18*	3.52 ± 0.17$^{\#\delta\delta}$

Results are expressed as mean ± SEM, n=6. * P < 0.05, ** P< 0.01 vs Control-chow; # P < 0.05, ##

P < 0.01 vs Control-HFD; δ P < 0.05, δδ P < 0.01 vs KYD-chow.

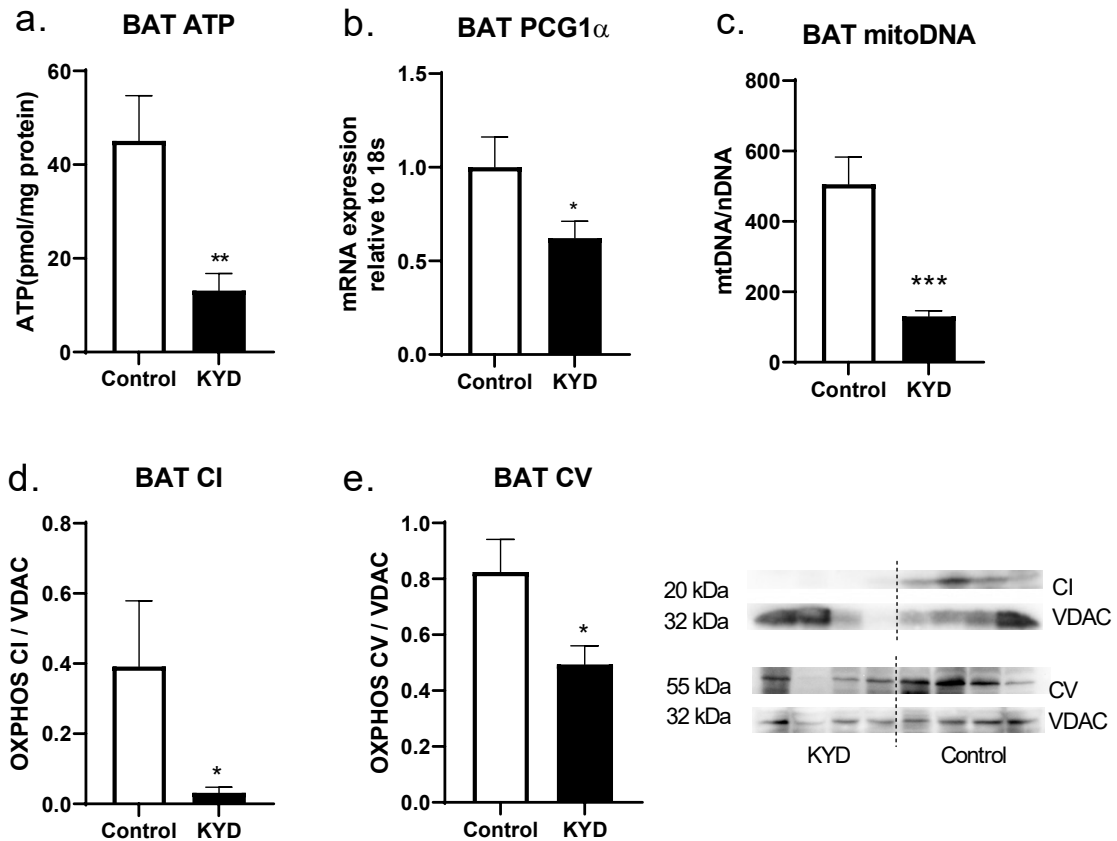HFD: high-fat diet; KYD: kidney yang deficiency; LDL: Low-Density Lipoprotein.

634
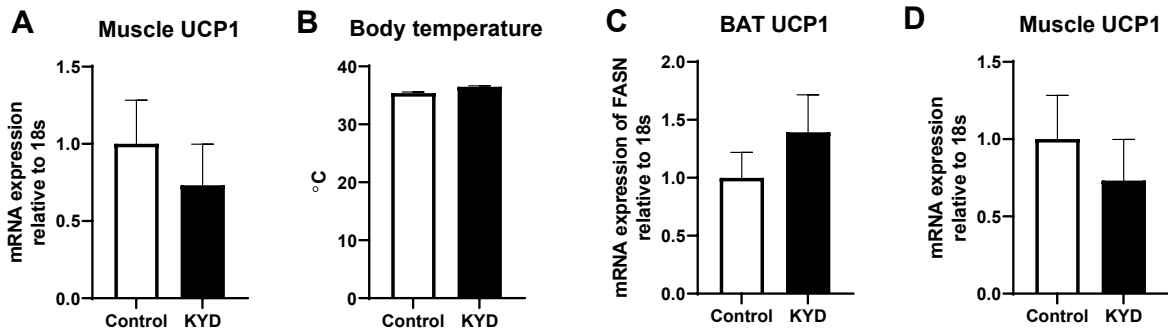
Figure 1: Hot plate test (a), body temperature (b), mRNA expression of uncoupling protein 1 (UCP1) in the brown adipose tissue (BAT, c) and skeletal muscle (d) in male offspring at 13 weeks. Results are expressed as mean ± SEM, n=6-10. * P < 0.05, ** P< 0.01. KYD: kidney yang deficiency;
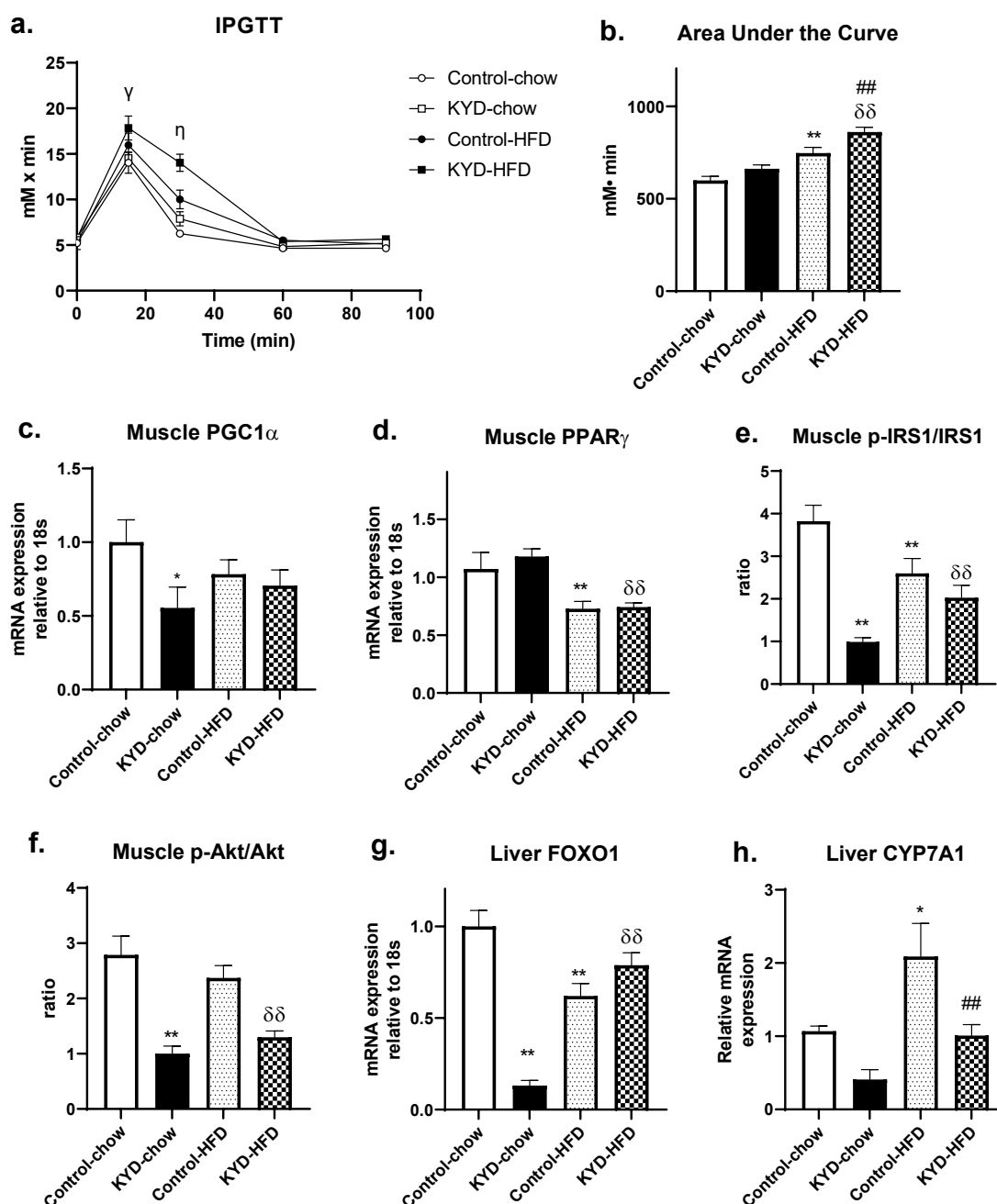

Figure 2: ATP levels (a), peroxisome proliferator-activated receptor gamma coactivator 1-alpha (PCG1α) mRNA expression (b), Mitochondrial DNA (mitoDNA) copy number (c), oxidative phosphorylation complexes CI (d) and CV (e) in the brown adipose tissue (BAT) in male offspring at 13 weeks. Results are expressed as mean ± SEM, n = 4-6. * P < 0.05, ** P< 0.01. KYD: kidney yang deficiency;
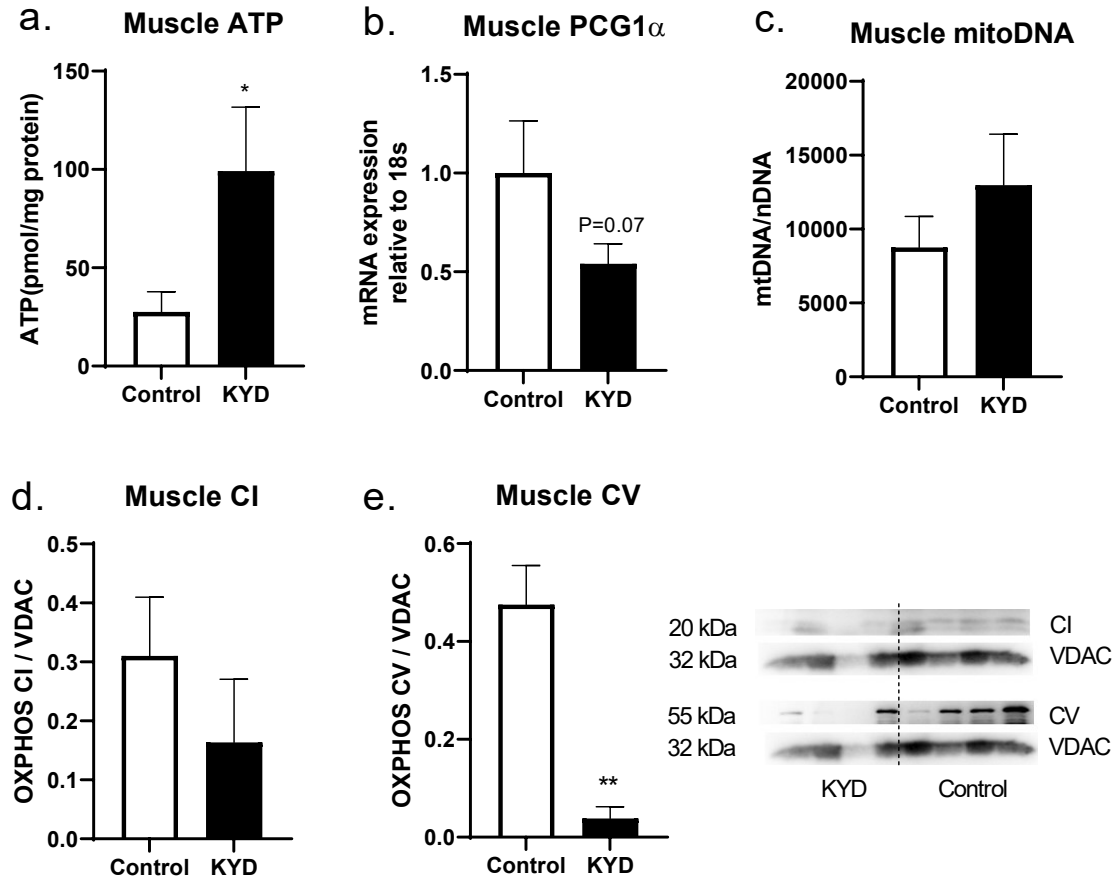
645

646 **Figure 3**: ATP levels (a), peroxisome proliferator-activated receptor gamma coactivator 1-alpha

647 (PCG1α) mRNA expression (b), Mitochondrial DNA (mitoDNA) copy number (c), oxidative

648 phosphorylation complexes CI (d) and CV (e) in the skeletal muscle in male offspring at 13 weeks.

649 Results are expressed as mean ± SEM, n = 4-6. * P < 0.05, ** P< 0.01. KYD: kidney yang deficiency;

650

Figure 4 Blood glucose level change during intraperitoneal glucose tolerance test (IPGTT, a) and area under the curve (b) of (a) in male offspring at 12 weeks. Peroxisome proliferator-activated receptor gamma coactivator 1-alpha (PCG1α, c) and Peroxisome proliferator-activated receptor gamma (PPARγ, d) mRNA expression, and ratios between p-insulin receptor substrate (IRS)1 and total IRS1 (e) and between p-protein kinase B (Akt) and total Akt (f) in the skeletal muscle, as well as mRNA expression of Forkhead box protein O (FOXO)1 (g) and Cholesterol 7 alpha-hydroxylase (CYP7A1, h) in the liver in chow and HFD-fed rats at 13 weeks. Results are expressed as mean ± SEM, n=6. γ P<0.05 KYD-chow vs KYD-HFD; η P< 0.01 Control-chow vs Control-HFD, KYD-chow vs KYD-HFD, Control-HFD vs KYD-HFD; * P < 0.05, ** P< 0.01 vs Control-chow; # P < 0.05, ## P < 0.01 vs Control-HFD; δ P < 0.05, δδ P < 0.01 vs KYD-chow. HFD: high-fat diet; KYD: kidney yang deficiency;

665
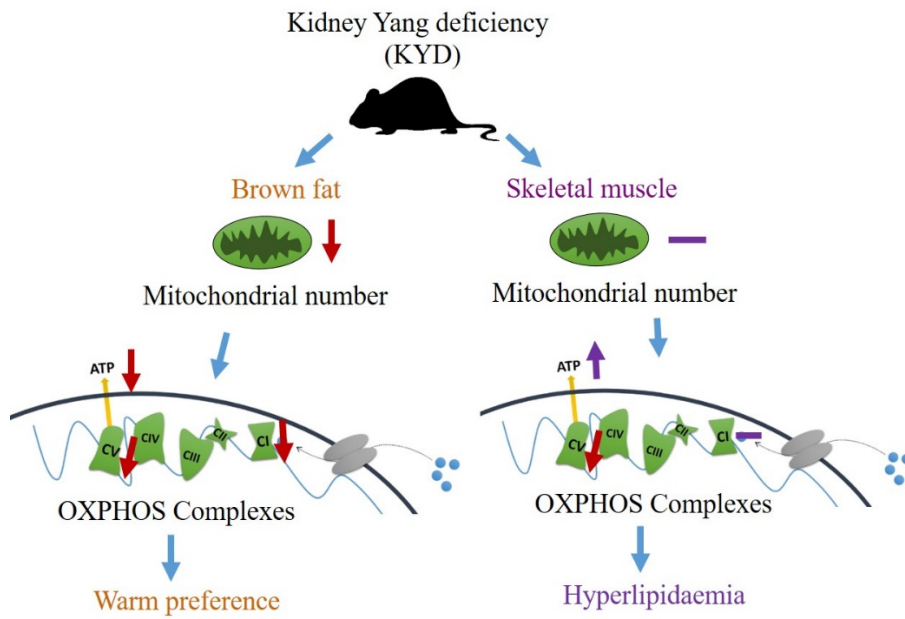
Figure 5: Working mechanism of the phenotype in Kidney Yang Deficiency (KYD). Mitochondrial
disorder in the brown fat leads to warm preference, whereas the compensation of mitochondrial
function in the skeletal muscle maintained body temp.

669